Osteoporosis and Sarcopenia 8 (2022) 112–122

Contents lists available at ScienceDirect

Osteoporosis and Sarcopenia

journal homepage: http://www.elsevier.com/locate/afos

Original article

Support vector machines are superior to principal components analysis for selecting the optimal bones' CT attenuations for opportunistic screening for osteoporosis using CT scans of the foot or ankle

Ronnie Sebro [a, b, *], Cynthia De la Garza-Ramos [a]

[a] Department of Radiology, Mayo Clinic, Jacksonville, FL, 32224, USA
[b] Center for Augmented Intelligence, Mayo Clinic, Jacksonville, FL, 32224, USA

ARTICLE INFO

Article history:
Received 25 January 2022
Received in revised form
14 May 2022
Accepted 1 September 2022
Available online 24 September 2022

Keywords:
Talus
Calcaneus
Navicular
Cuneiform
Cuboid

ABSTRACT

Objectives: To use the computed tomography (CT) attenuation of the foot and ankle bones for opportunistic screening for osteoporosis.
Methods: Retrospective study of 163 consecutive patients from a tertiary care academic center who underwent CT scans of the foot or ankle and dual-energy X-ray absorptiometry (DXA) within 1 year of each other. Volumetric segmentation of each bone of the foot and ankle was done in 3D Slicer to obtain the mean CT attenuation. Pearson's correlations were used to correlate the CT attenuations with each other and with DXA measurements. Support vector machines (SVM) with various kernels and principal components analysis (PCA) were used to predict osteoporosis and osteopenia/osteoporosis in training/validation and test datasets.
Results: CT attenuation measurements at the talus, calcaneus, navicular, cuboid, and cuneiforms were correlated with each other and positively correlated with BMD T-scores at the L1-4 lumbar spine, hip, and femoral neck; however, there was no significant correlation with the L1-4 trabecular bone scores. A CT attenuation threshold of 143.2 Hounsfield units (HU) of the calcaneus was best for detection of osteoporosis in the training/validation dataset. SVMs with radial basis function (RBF) kernels were significantly better than the PCA model and the calcaneus for predicting osteoporosis in the test dataset.
Conclusions: Opportunistic screening for osteoporosis is possible using the CT attenuation of the foot and ankle bones. SVMs with RBF using all bones is more accurate than the CT attenuation of the calcaneus.

1. Introduction

Bone mineral density (BMD) decreases with age, especially in post-menopausal women [1–4]. Diminished BMD results in osteoporosis, osteopenia, and increased risk of insufficiency/osteoporotic fractures including fractures of the spine, forearm, hips and calcaneus [5–10]. Dual-energy X-ray absorptiometry (DXA) is considered the gold standard for measuring BMD and for the diagnosis of osteoporosis and osteopenia [11]. DXA BMD measurements are typically obtained at the L1-L4 lumbar spine, femoral neck, and total hip [12]. Using the World Health Organization (WHO) diagnostic guidelines [13], patients with their lowest DXA BMD T-scores less than or equal to −2.5 are diagnosed as osteoporotic; patients with their lowest BMD T-scores between −1 and −2.5 are diagnosed as osteopenic; and patients with their lowest BMD T-scores greater than or equal to −1 are considered to have normal BMD [13]. The trabecular bone score (TBS) obtained from DXA is a measure of bone texture, is correlated with bone microarchitecture and is a marker for the risk of osteoporosis [14]. TBS provide complementary information to BMD T-scores for the estimation of fracture risk [14,15].

More recent data has shown that opportunistic screening for osteoporosis and osteopenia can be accomplished using the computed tomography (CT) attenuation of the lumbar and thoracic spine from CT scans of the chest, abdomen, and pelvis [16,17]. BMD

* Corresponding author. Department of Radiology, Mayo Clinic, Jacksonville, FL, 32224, USA.
E-mail address: rsebro@gmail.com (R. Sebro).
Peer review under responsibility of The Korean Society of Osteoporosis.

https://doi.org/10.1016/j.afos.2022.09.002

measurements are sometimes obtained using quantitative ultrasound at the calcaneus [18,19]. Because the quantitative ultrasound BMD measurements at the calcaneus can be used to predict osteoporotic fractures, we hypothesized that the CT attenuation of the calcaneus would be correlated with DXA BMD measurements. We also hypothesized that the CT attenuation of the other bones visualized on CT scans of the foot/ankle would be predictive of DXA BMD measurements.

The aims of this study are to (1) evaluate the correlations between the CT attenuation measurements of the foot and ankle bones including the talus, calcaneus, navicular, cuboid, medial, middle, and lateral cuneiforms in patients aged 50 years or older; (2) to evaluate the correlations between the CT attenuation of the foot and ankle bones and DXA BMD and L1-L4 TBS measurements; (3) to evaluate the predictive ability of the CT attenuation of each of the foot and ankle bones to predict (a) osteoporosis using the WHO guidelines, (b) osteopenia/osteoporosis using the WHO guidelines, (c) a femoral neck BMD T-score ≤ -2.5, and (d) femoral neck BMD T-score < -1; and (4) to use machine learning (ML) including support vector machines (SVMs) and principal components analysis (PCA) using the CT attenuation of the foot and ankle bones to predict (a) osteoporosis using the WHO guidelines, (b) osteopenia/osteoporosis using the WHO guidelines, (c) a femoral neck BMD T-score ≤ -2.5 and (d) femoral neck BMD T-score < -1.

2. Methods

This study was approved by the ethical review board of this institution (#21-000724). A waiver for signed informed consent from each patient was obtained due to the retrospective nature of the study. Data was collected in accordance with the Health Insurance Portability and Accountability Act of 1996. Medical research was done in accordance with the Declaration of Helsinki ethical principles for medical research involving human subjects.

Patients were included if they were aged 50 years or older, had a complete DXA study of the L1-L4 lumbar spine, femoral neck, total hip, and TBS of the L1-L4 lumbar spine and a CT scan of the foot/ankle within 1 year of each other. Patients were excluded if they had prior surgery with hardware in the lumbar spine, hip, or foot/ankle, as this could alter the CT attenuation of the bones. All patients were imaged between January 1st, 2015, and November 30th, 2021.

2.1. DXA scanners

DXA scans were performed using General Electric (GE) (Waukesha, Wisconsin, USA) Luna iDXA. The L1-L4 BMD, L1-L4 BMD T-scores and L1-L4 BMD TBS, femoral neck BMD, femoral neck BMD T-scores, total hip BMD, total hip BMD T-scores were recorded. Patient age, gender, height, weight, and body mass index (BMI) at the time of the DXA study were recorded. The least significant change (LSC) for L1-L4 BMD measurements was 0.028 g/cm^2 and the LSC for the hip BMD measurements was 0.028 g/cm^2.

2.2. CT scanner protocol and CT attenuation measurements

CT scans of the foot or ankle were performed using Siemens Definition AS and Siemens Somatom Force (Siemens Healthineers, Erlangen, Germany). CT scans were performed at 120 kVp, 250 mA, and acquired at 0.4 mm slice thickness in the axial plane and subsequently reconstructed in the coronal and sagittal planes at 1 mm slice thickness. No intravenous contrast was given. There were 86 CT scans of the ankle and 77 CT scans of the foot. CT scans of the foot or ankle used the same imaging parameters but differed in the size of the field of view - the CT scans of the ankle terminated at the mid-metatarsals, whereas the CT scans of the foot included up to the distal tibia.

All Digital Imaging and Communications in Medicine (DICOM) images from each study were anonymized, downloaded, and imported into 3D Slicer [20]. 3D Slicer was used to segment the distal third of the tibia, ultradistal (UD) tibia (metaphysis and epiphysis), tibial 33%, distal fibula, UD fibula, fibula 33%, talus, calcaneus, navicular, cuboid, medial, middle, and lateral cuneiforms, and proximal third of the first through fifth metatarsals to obtain the mean CT attenuation values of these bones. Semi-automatic volumetric segmentation was performed by a research assistant who was trained and supervised by a fellowship-trained musculoskeletal radiologist with over 8 years of experience. The osseous cortex, and bone islands/enostoses were excluded from the segmentations, since these could affect the CT attenuation of each bone (Fig. 1) [21]. The mean CT attenuation of each bone was recorded and used in the analysis.

Because of the variable CT scanning fields of view for each study, there was greater than 20% missing data for the distal tibial, fibular, and proximal third of the first through fifth metatarsals measurements, so these variables were excluded from the machine learning analysis.

We considered the CT attenuation of all bones (bones with fractures, degenerative changes, and arthritis) because this simulates a real-world experience, since approximately 50% of studies were performed for arthritis/degenerative changes and the other 50% of studies were performed in the setting of trauma to exclude fractures. Since bone marrow edema and hemorrhage related to fractures may affect the CT attenuation of a bone with a fracture [22], we repeated the analyses excluding all bones with any fractures and present these results in Supplementary Tables 1 and 2 However, limiting the study to patients with no fractures made the study sample size too small for machine learning approaches.

2.3. Statistical analysis

The study sample was randomly divided into training/validation (63%; N = 103) and test datasets (37%; N = 60). A testing dataset with a sample size of 60 patients was determined to have 80% power with a Type I error rate of 5% to detect a difference between two receiver operator characteristic (ROC) curves if the first ROC curve has an area under the receiver operator curve (AUC) of 0.80 and the second ROC curve has an AUC of 0.65, assuming 20% of patients are osteoporotic and 80% are non-osteoporotic.

Summary statistics for the clinical and demographic variables, including age, gender, height, weight, and body mass index (BMI) were calculated in the training/validation and test datasets. Quantitative and qualitative clinical and demographic variables were compared between the training/validation dataset and test dataset using t-tests with unequal variances and Fisher's exact tests respectively.

Pearson's and Spearman's correlation coefficients were used to assess the correlations between the CT attenuation measurements at each osseous site and hierarchical clustering was used to cluster the Pearson's correlations between each osseous site.

Pearson's correlation coefficients were also used to evaluate the correlation between the CT attenuation measurements at each osseous site and the DXA measurements (L1-L4 BMD, L1-L4 BMD T-score, L1-L4 TBS, femoral neck BMD, femoral neck BMD T-score, total hip BMD, total hip BMD T-score). Pearson's correlation coefficients were also used to evaluate the correlations between the CT attenuation measurements at each osseous site and the clinical/demographic variables.

Univariate ROC analyses were done using the CT attenuation of each bone to predict (a) osteoporosis using the WHO guidelines, (b)

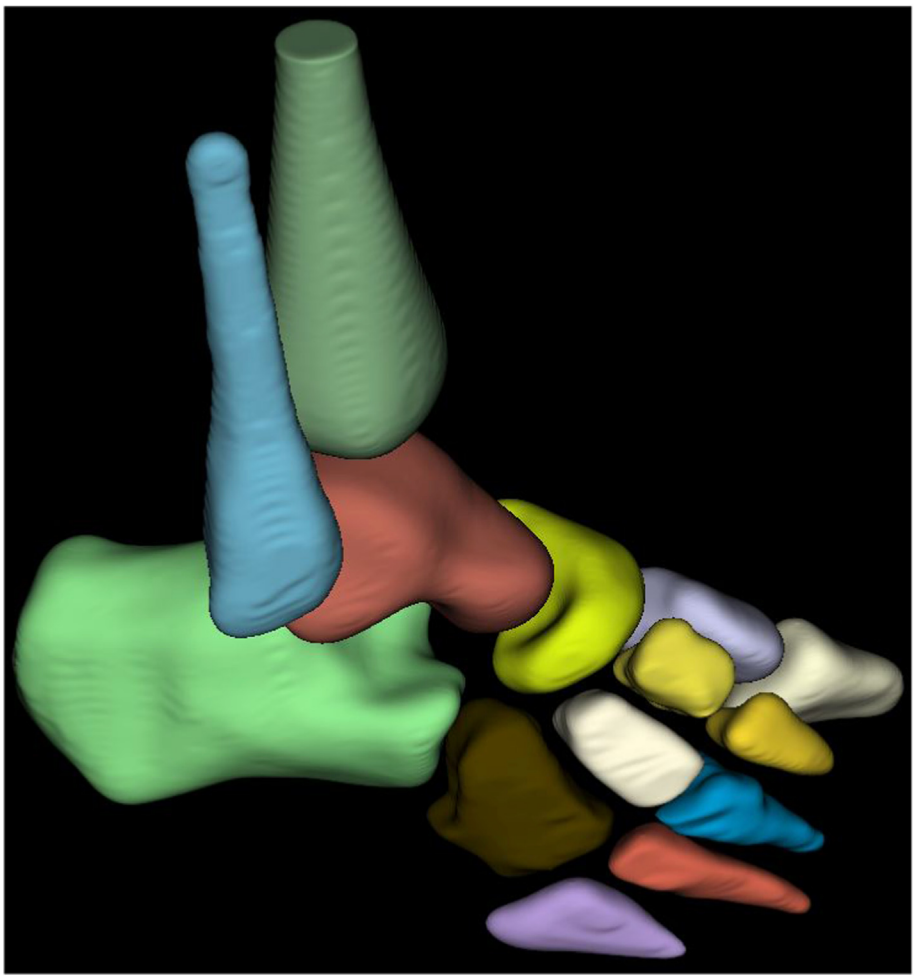

Fig. 1. Volumetric segmentation of the foot and ankle bones.

osteopenia/osteoporosis using the WHO guidelines, (c) a femoral neck BMD T-score ≤ -2.5, and (d) a femoral neck BMD T-score < -1 in the training/validation dataset. We evaluated the femoral neck BMD T-scores because these BMD T-scores are thought to be less likely affected by degenerative changes at the spine and hip. The performance of the mean CT attenuation of each osseous site was assessed using the AUC, sensitivity, specificity, accuracy, positive predictive value, and negative predictive value.

Because manually measuring the CT attenuation of all the osseous sites on CT will be time intensive for clinicians unless fully automated, we tried to find the optimal combination of the CT attenuation of osseous sites to best predict (a) osteoporosis based on WHO guidelines, (b) osteoporosis/osteopenia based on WHO guidelines, (c) femoral neck BMD T-score ≤ -2.5, and (d) femoral neck BMD T-score < -1. For these multivariable analyses we utilized the following variables: age, gender, height, weight, BMI, and the CT attenuation of the talus, calcaneus, navicular, cuboid, medial, intermediate, and lateral cuneiforms.

SVMs in machine learning, are supervised learning models with associated learning algorithms that can be used to analyze data for classification. We used C-classification with 3 different kernels: a linear kernel, a sigmoid kernel, and a radial basis function (RBF) kernel.

Linear kernel, $K(x, y) = x.y$ [Equation 1]

RBF kernel, $K(x, y) = e^{\left(||x-y||^2\right)/2\sigma^2}$ [Equation 2]

Sigmoid kernel, $K(x, y) = \tanh(\upsilon(x.y) + c)$ [Equation 3]

We used SVMs with each of the different kernels to classify patients as (a) osteoporotic or (b) osteopenic/osteoporotic, both using the WHO guidelines, (c) having a femoral neck BMD T-score ≤ -2.5, and (d) as having a femoral neck BMD T-score < -1. We used 10-fold cross validation to optimize tuning in each model in the training/validation dataset. The tuning for each SVM was performed over epsilon ranges from 0 to 1 by 0.05 increments, with cost values ranging from 1 to 8 by increments of 1. Models with different kernels were compared using DeLong's test and the model in which the kernel had the highest AUC in the training/validation dataset was selected as the best model. We then evaluated the performance of the best SVM model in the test dataset.

PCA is a statistical technique commonly used for dimensionality reduction by projecting each data point onto only the first few principal components (PCs) to obtain lower-dimensional data while preserving as much of the variance in the data as possible. PCA can be used to differentiate clusters and for making predictive models. All quantitative variables (age, height, weight, BMI, and the CT attenuations of the talus, calcaneus, navicular, cuboid, lateral cuneiform, intermediate cuneiform, and medial cuneiform) were centered and scaled before being used in the PCA. PCA was used to

separate patients with osteoporosis from non-osteoporotic patients in the training/validation dataset, and the PCs from this model were saved. The PCs were then used in a multivariable logistic regression model to classify the patients as (a) osteoporotic versus non-osteoporotic using the WHO guidelines and using all 12 PCs. This model was used to predict the probabilities of being osteoporotic versus non-osteoporotic in the test dataset.

We repeated the PCA, this time separating (b) patients with osteopenia/osteoporosis from normal patients. The PCs from this model were saved and projected onto the test dataset to classify the patients as osteopenic/osteoporotic versus normal. We used PCA to (c) classify patients as having a femoral neck BMD T-score ≤ -2.5 or femoral neck BMD T-score > -2.5 in the training/validation datasets and then the PCs from this model were used in a multivariable logistic regression model and evaluated in the test dataset to classify the patients in the test dataset as having a femoral neck BMD T-score ≤ -2.5 or having a femoral neck BMD T-score > -2.5. PCA was also used to (d) differentiate patients with femoral neck BMD T-score < -1 from patients with femoral neck BMD ≥ -1 in the training/validation dataset. These PCs were then used in a multivariable logistic regression model to classify the patients as (d) femoral neck BMD T-score < -1 using all 12 PCs. This model was used to predict the probabilities of femoral neck BMD T-score < -1 versus femoral neck BMD T-score ≥ -1 in the test dataset.

The performance (sensitivity, specificity, accuracy, positive predictive value, and negative predictive value) of the SVM models and PCA models in the test dataset were evaluated and compared to the univariate models using the CT attenuation of the calcaneus and medial cuneiform using DeLong's test. The calcaneus has been historically used as the bone evaluated in the foot and ankle for screening for osteoporosis [18,19]. In addition, a recent study showed that the distal dorsal lateral aspect of medial cuneiform had higher CT attenuation and was denser than all other sites in the medial cuneiform and suggested that this site should be used for hardware implantation [23]. Therefore, we compared the performance of each machine learning model to the performance of the CT attenuation of the calcaneus and the medial cuneiform, and since the medial cuneiform is often used for hardware implantation, we compared the predictive properties of this bone compared to the others.

Statistics were carried out using *Rv4.1.2* using the *pROC*, *e1071*, and *prcomp* packages and all test statistics were two-sided. We considered P-values < 0.05 to be statistically significant.

3. Results

The study comprised of 163 patients with a median age of 64.0 years (range 50.0–86.0 years) and 19.0% were male. Table 1 shows clinical and demographic characteristics of the study patients. There were no significant differences between the training/validation and test datasets. Fig. 2 shows box and whisker plots of the distributions of the mean CT attenuation for each osseous site by diagnosis (osteoporosis, osteopenia, and normal). The mean CT attenuation of each bone was significantly lower in patients with osteoporosis than patients with osteopenia ($P < 0.001$ for all) and the mean CT attenuation of each bone was significantly lower in patients with osteopenia than normal patients ($P < 0.001$ for all).

We found strong positive Pearson's correlations between the mean CT attenuation at each osseous site, ranging from 0.56 between the cuboid and the navicular, to 0.85 between the talus and the navicular (Table 2). Fig. 3 shows that the bones along the primary weight bearing axis (medial longitudinal arch) of the foot (talus, navicular, and medial cuneiform) had more similar CT attenuations than the bones along the transverse arch (lateral cuneiform and cuboid).

There were strong positive correlations between the mean CT attenuation of each osseous site and DXA measurements (Table 3). The CT attenuation of the calcaneus ($r = 0.33$, $P < 0.001$), had the strongest positive correlation with the L1-L4 BMD T-score, whereas the CT attenuation of the cuboid ($r = 0.16$, $P = 0.047$) had the weakest positive correlation with the L1-L4 BMD T-score (Table 3). We found that the CT attenuation of the talus ($r = 0.43$, $P < 0.001$) had the strongest positive correlation with the femoral neck BMD T-score, whereas the CT attenuation of the cuboid ($r = 0.28$, $P < 0.001$) had the weakest correlation with the femoral neck BMD T-score. Similarly, the total hip BMD T-score most strongly correlated with the CT attenuation of the talus ($r = 0.52$, $P < 0.001$) and had the weakest correlation with the CT attenuation of the cuboid ($r = 0.40$, $P < 0.001$). The L1-L4 TBS had the strongest positive correlation with the CT attenuation of the medial cuneiform ($r = 0.22$, $P = 0.051$), and weakest positive correlation with the CT attenuation of the navicular ($r = 0.09$, $P = 0.442$), however, the L1-L4 TBS was not significantly correlated with any CT attenuation measurement. Age negatively correlated with the CT attenuation at each bone except the calcaneus, however, none of these correlations was statistically significant. BMI and weight were statistically significantly positively correlated with the CT attenuation of the calcaneus, talus, and navicular (Table 3).

ROC curves were used to predict (a) osteoporosis based on WHO guidelines, (b) osteoporosis/osteopenia based on WHO guidelines, (c) femoral neck BMD T-score ≤ -2.5, and (d) femoral neck BMD T-score < -1 using the mean CT attenuation of each osseous site (talus, calcaneus, navicular, cuboid, medial, middle, and lateral cuneiforms).

We found that a CT attenuation of the talus at a threshold of 284.0 HU had the highest accuracy to predict osteoporosis in the training/validation dataset (accuracy = 0.728, sensitivity = 0.556, specificity = 0.789, and AUC = 0.698), whereas the CT attenuation of the lateral cuneiform at a threshold of 264.6 HU had the lowest accuracy (accuracy = 0.602, sensitivity = 0.852, specificity = 0.513, and AUC = 0.686) (Table 4) (Supplementary Fig. 1). A CT attenuation threshold of 327.3 HU at the medial cuneiform had the highest accuracy to predict osteopenia/osteoporosis (accuracy = 0.825, sensitivity = 0.890, specificity = 0.571, and AUC = 0.740) while a CT attenuation threshold of 380.2 HU at the intermediate cuneiform had the lowest accuracy to predict osteopenia/osteoporosis (accuracy = 0.631, sensitivity = 0.585, specificity = 0.810, and AUC = 0.756) (Supplementary Fig. 2). When predicting femoral neck BMD T-scores ≤ -2.5 in the training/validation dataset, we found that a CT attenuation threshold of 201.9 HU at the lateral cuneiform had the highest accuracy (accuracy = 0.786, sensitivity = 0.538, specificity = 0.822, and AUC = 0.666), while a CT attenuation threshold of 424.9 HU at the intermediate cuneiform had the lowest accuracy (accuracy = 0.447, sensitivity = 0.923, specificity = 0.378, and AUC = 0.631) (Supplementary Fig. 3). We found that a CT attenuation threshold of 349.6 at the talus had the highest accuracy (accuracy = 0.738, sensitivity = 0.786, specificity = 0.636, and AUC = 0.750) to predict femoral neck BMD T-scores < -1 in the training/validation dataset, while a CT attenuation threshold of 115.5 HU at the cuboid had lowest accuracy (accuracy = 0.612, sensitivity = 0.443, specificity = 0.939, and AUC = 0.702) (Supplementary Fig. 4).

We found that the RBF kernel (AUC = 0.942) was better than the sigmoid (AUC = 0.568) and linear (AUC = 0.819) SVMs in the training/validation dataset to predict osteoporosis. When predicting osteopenia/osteoporosis, we also found that the RBF kernel (AUC = 0.968) was better than the sigmoid (AUC = 0.570), and linear kernel (AUC = 0.888) SVMs in the training/validation dataset. We also found that the RBF kernel (AUC = 0.964) was better than the sigmoid (AUC = 0.568) and linear kernel (AUC = 0.821) SVMs

Table 1
Comparison between training/validation and test datasets.

Variable	All (N = 163)	Training/validation dataset (N = 103)	Test dataset (N = 60)	P-value
Age, yrs	65.1 (7.8)	64.9 (8.2)	65.3 (7.1)	0.730
Race/ethnicity				
Black	1 (0.6%)	1 (1.0%)	0 (0.0%)	0.792
Hispanic	4 (2.5%)	3 (2.9%)	1 (1.7%)	
Other	2 (1.2%)	2 (1.9%)	0 (0.0%)	
White	156 (95.7%)	97 (94.2%)	59 (98.3%)	
Gender, Female	132 (81.0%)	83 (80.6%)	49 (81.7%)	1.00
Height, m	1.65 (0.08)	1.66 (0.08)	1.64 (0.09)	0.262
Weight, kg	80.1 (19.5)	80.9 (19.4)	78.6 (19.6)	0.474
BMI, kg/m^2	29.3 (6.8)	29.4 (6.8)	29.1 (6.9)	0.792
Indication				
Trauma	86 (52.8%)	51 (49.5%)	35 (58.3%)	0.330
Arthritis	77 (47.2%)	52 (50.5%)	25 (41.7%)	
Fractures				
Tibia	49 (30.1%)	30 (29.4%)	19 (31.7%)	0.942
Fibula	51 (31.3%)	31 (30.1%)	20 (33.3%)	
Talus	9 (5.5%)	4 (3.9%)	5 (8.3%)	
Calcaneus	13 (8.0%)	6 (5.8%)	7 (11.7%)	
Cuboid	8 (4.9%)	5 (4.9%)	3 (5.0%)	
Navicular	4 (2.5%)	2 (1.9%)	2 (3.3%)	
Medial cuneiform	5 (3.1%)	4 (3.9%)	1 (1.7%)	
Middle cuneiform	4 (2.5%)	2 (1.9%)	2 (3.3%)	
Lateral cuneiform	6 (3.7%)	4 (3.9%)	2 (3.3%)	
1st metatarsal	5 (3.1%)	4 (3.9%)	1 (1.7%)	
2nd metatarsal	9 (5.5%)	5 (4.9%)	4 (6.7%)	
3rd metatarsal	9 (5.5%)	7 (6.8%)	2 (3.3%)	
4th metatarsal	9 (5.5%)	7 (6.8%)	2 (3.3%)	
5th metatarsal	8 (4.9%)	5 (4.9%)	3 (5.0%)	
Diagnosis				
Osteoporosis	42 (%)	27 (%)	15 (%)	0.908
Osteopenia	86 (%)	55 (%)	31 (%)	
Normal	35 (%)	21 (%)	14 (%)	

BMI, body mass index; osteoporosis, minimum BMD T-score ≤ -2.5; osteopenia – $-2.5 <$ minimum BMD T-score < -1; normal – minimum BMD T-score ≥ -1.

for predicting femoral neck BMD T-scores ≤ -2.5 in the training/validation dataset. Additionally, we found that the best kernel for predicting femoral neck BMD T-scores < -1 was the RBF kernel (AUC = 0.923), which was better than the sigmoid (AUC = 0.628) and linear (AUC = 0.857) kernels.

PCA in the training/validation dataset showed that the first PC loadings were heaviest on the CT attenuations of the calcaneus, talus, navicular, cuboid, lateral, intermediate, and medial cuneiforms; the second PC loadings were heaviest on gender, height, weight, and BMI; the third PC loadings were heaviest on BMI and weight; and the fourth PC loadings were heaviest on age. Approximately 45.4% of the variance was explained by PC1, 15.9% by PC2, 12.8% by PC3 and 8.5% by PC4.

When we evaluated the performance of the univariate, SVM with a RBF kernel and PCA models in the test dataset to predict osteoporosis, we found that the SVM with a RBF kernel was the model with the highest AUC (accuracy = 0.767, sensitivity = 0.867, specificity = 0.733, and AUC = 0.867) and this model had a higher AUC than the univariate model using the CT attenuation threshold of 143.243 HU at the calcaneus (AUC = 0.356; P < 0.001), had a higher AUC than the univariate model using the CT attenuation threshold of 260.755 HU at the medial cuneiform (AUC = 0.622; P < 0.001), and a higher AUC than the PCA model (AUC = 0.733; P = 0.028) (Table 5) (Supplementary Fig. 5). The SVM with the RBF kernel (AUC = 0.783) was also better than the PCA model (AUC = 0.635; P = 0.048) and better than the univariate model using a CT attenuation of 327.331 HU at the medial cuneiform (AUC = 0.318, P < 0.001) but not significantly better than the univariate model using a CT attenuation of 141.054 HU at the calcaneus (AUC = 0.708, P = 0.444) to differentiate patients with osteopenia/osteoporosis from patients with normal BMD (Supplementary Fig. 6).

The analysis also showed that a SVM with RBF kernel (AUC = 0.750) was better than the PCA model (AUC = 0.524, P = 0.003) but not significantly better than the univariate model using a CT attenuation of 116.188 HU at the calcaneus (AUC = 0.708, P = 0.444) or the univariate model using a CT attenuation of 257.7 HU at the medial cuneiform (AUC = 0.582, P = 0.148) to identify patients with femoral neck BMD ≤ -2.5 (Table 5) (Supplementary Fig. 7). When predicting femoral neck BMD < -1, we found that the SVM with RBF kernel (AUC = 0.766) was better than the PCA model (AUC = 0.590; P = 0.003) and the univariate models using a CT attenuation of 122.043 HU at the calcaneus (AUC = 0.382; P < 0.001) and using a CT attenuation of 245.128 HU at the medial cuneiform (AUC = 0.424; P = 0.002) (Supplementary Fig. 8).

Patients with fractures were slightly more likely to have osteoporosis, but this was not statistically significant (P = 0.592). We found that the performance of the CT attenuations of the individual bones improved when we excluded bones with fractures (Supplementary Table 1 and Supplementary Table 2), however, the performance was substantially worse than the SVM with RBF models.

4. Discussion

We found that there were strong positive correlations between the CT attenuation measurements of the foot and ankle bones including the talus, calcaneus, navicular, cuboid, medial, intermediate, and lateral cuneiforms in patients aged 50 years or older. There were positive correlations between the CT attenuations of the foot and ankle bones and DXA BMD measurements, but no significant correlations between the CT attenuations of the foot and ankle bones and L1-L4 TBS measurements. The CT attenuation of each bone was predictive of osteoporosis and osteopenia/osteoporosis,

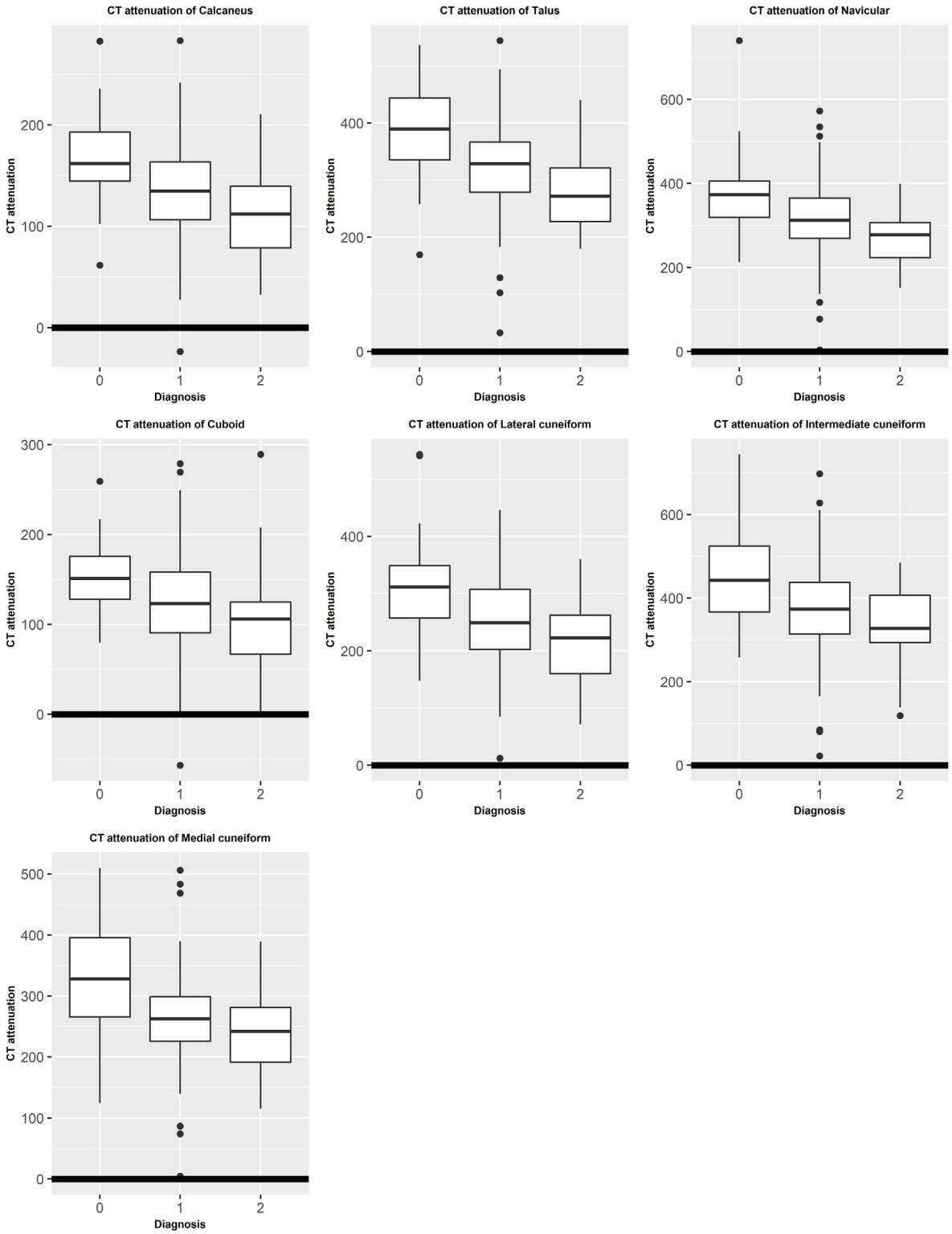

Fig. 2. Box and whisker plots of the distribution of the mean CT attenuation of each bone
Fig. 2 caption: 0 – Normal. 1 – Osteopenia. 2 - Osteoporosis.

however, the CT attenuation of the calcaneus at a threshold of 143.2 HU was best to predict osteoporosis and the CT attenuation of the talus at a threshold of 362.2 HU was best to predict osteopenia/osteoporosis. Machine learning showed that SVMs with RBF kernels were better than SVMs with other kernels (linear and sigmoid) for predicting whether a patient had (a) osteoporosis, (b) osteopenia/osteoporosis, (c) femoral neck BMD ≤ -2.5, and (d) femoral neck BMD < -1. Although PCA was predictive of whether a patient had (a) osteoporosis, (b) osteopenia/osteoporosis, (c) femoral neck BMD ≤ -2.5, and (d) femoral neck BMD < -1, we found that in

Table 2
Correlations between CT attenuations at osseous sites.

Males/Females	Calcaneus	Talus	Navicular	Cuboid	Lateral cuneiform	Intermediate cuneiform	Medial cuneiform
Calcaneus	–	0.80 ***	0.73 ***	0.67 ***	0.61 ***	0.64 ***	0.69 ***
Talus	0.84 ***	–	0.84 ***	0.69 ***	0.66 ***	0.74 ***	0.81 ***
Navicular	0.78 ***	0.85 ***	–	0.61 ***	0.69 ***	0.74 ***	0.80 ***
Cuboid	0.67 ***	0.65 ***	0.57 ***	–	0.57 ***	0.59 ***	0.63 ***
Lateral cuneiform	0.60 ***	0.68 ***	0.64 ***	0.61 ***	–	0.66 ***	0.66 ***
Intermediate cuneiform	0.67 ***	0.77 ***	0.78 ***	0.58 ***	0.68 ***	–	0.74 ***
Medial cuneiform	0.76 ***	0.84 ***	0.82 ***	0.67 ***	0.69 ***	0.78 ***	–

Upper diagonal – Spearman's correlations.
Lower diagonal – Pearson's correlations.
*** P-value < 0.001.
** 0.001 ≤ P-value < 0.01.
* 0.01 ≤ P-value < 0.05.

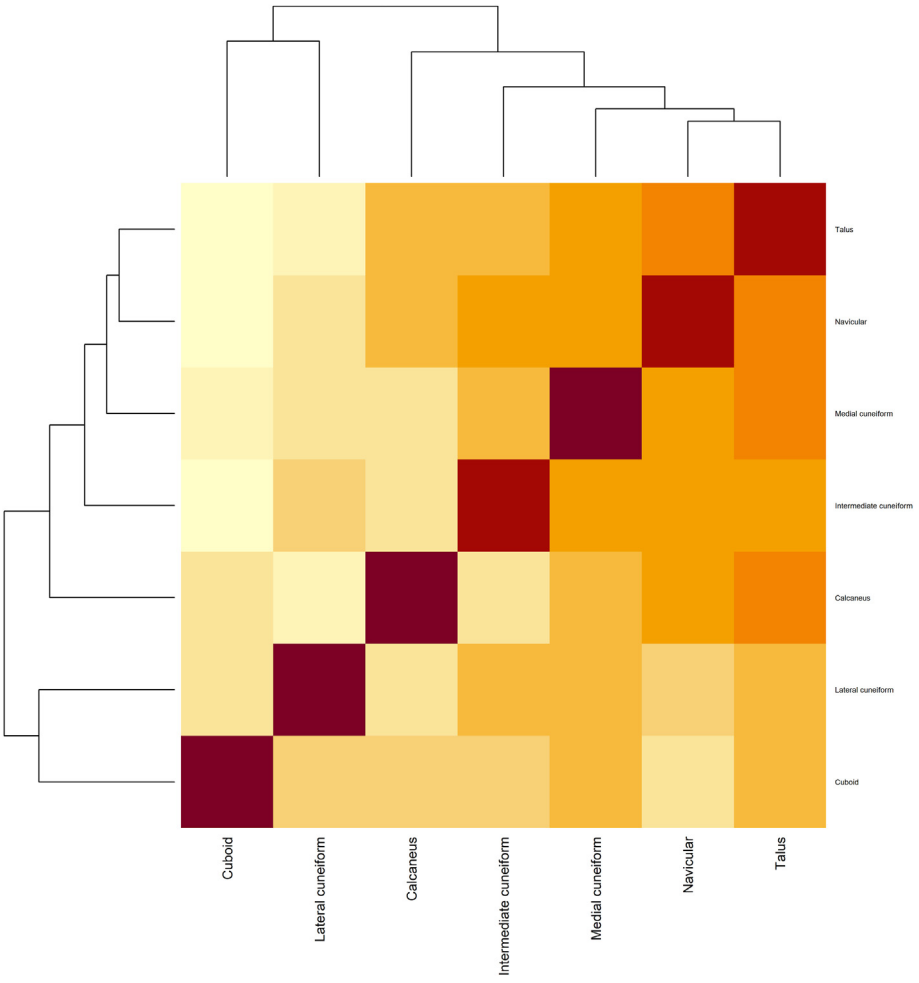

Fig. 3. Hierarchical clustering of the correlations between the CT attenuations of the foot and ankle bones.

general the SVM with RBF performed better for these classification tasks.

We show that the CT attenuation of several of the bones of the foot and ankle are highly correlated. Our study shows that opportunistic screening for osteoporosis and osteopenia can be done from CT scans of the foot and ankle, but more importantly, that utilizing the CT attenuation of multiple bones is far more informative than the CT attenuation of a single bone. In addition, we show that although PCA was informative for diagnosing osteoporosis and osteopenia, we find that SVMs with RBF kernels had

Table 3
Correlations between CT attenuation at different bony sites and DXA/clinical/demographic measurements.

Variable	Calcaneus	Talus	Navicular	Cuboid	Lateral cuneiform	Intermediate cuneiform	Medial cuneiform
L1-L4 BMD	0.37 ***	0.31 ***	0.30 ***	0.20 *	0.25 ***	0.21 **	0.27 ***
L1-L4 BMD T-score	0.36 ***	0.32 ***	0.30 ***	0.18 *	0.27 ***	0.20 **	0.25 **
L1-L4 TBS (N = 81)	0.21	0.12	0.09	0.18	0.16	0.11	0.22
Femoral neck BMD	0.39 ***	0.36 ***	0.35 ***	0.24 **	0.26 ***	0.31 ***	0.33 ***
Femoral neck BMD T-score	0.41 ***	0.43 ***	0.41 ***	0.28 ***	0.37 ***	0.37 ***	0.35 ***
Total hip BMD	0.56 ***	0.53 ***	0.47 ***	0.40 ***	0.46 ***	0.42 ***	0.43 ***
Total hip BMD T-score	0.54 ***	0.52 ***	0.46 ***	0.41 ***	0.47 ***	0.41 ***	0.41 ***
Age	0.03	−0.11	−0.06	−0.04	−0.02	−0.11	−0.06
Height	0.05	0.13	0.08	0.13	0.10	0.19 *	0.13
Weight	0.22 **	0.20 *	0.22 **	0.17 *	0.14	0.13	0.11
BMI	0.20 *	0.15	0.18 *	0.12	0.11	0.05	0.06

*** P-value < 0.001.
** 0.001 ≤ P-value < 0.01.
* 0.01 ≤ P-value < 0.05.
TBS – trabecular bone score.

higher AUCs and were more accurate.

A prior study by Cohen et al [24] investigating the use of the CT attenuation of L1-L4 for predicting osteoporosis and osteopenia showed that a CT attenuation threshold of 121 HU had a sensitivity of 74%, specificity of 61% and AUC of 0.764 to predict osteoporosis. This study also showed that a CT attenuation of 149 HU had a sensitivity of 76%, specificity of 74% and AUC of 0.815 to predict osteoporosis/osteopenia. Our results using a SVM with RBF are surprisingly similar. The SVM model had a sensitivity of 86.7%, specificity of 77.3% and AUC of 0.867 to predict osteoporosis; and had a sensitivity of 69.6%, specificity of 85.7% and AUC of 0.783 to predict osteopenia/osteoporosis in the test datasets. The performance of the CT attenuation of the individual bones (calcaneus, medial cuneiform) was worse for several reasons: the first reason is that the diagnosis of osteoporosis/osteopenia is based on DXA measurements of the lumbar spine and hips. The CT attenuation measurements of the lumbar spine and hips are probably most correlated with the DXA measurements of these same regions (the lumbar spine and hips). The second reason is that there are far more CT studies of the lumbar spine/abdomen and pelvis than CT studies of the foot or ankle performed each day. This means that there is far more data available to train a model using CT scans of the lumbar spine than CT scans of the foot or ankle. The model performance is dependent on having a large enough sample size to train the model. Finally, we included cases with degenerative changes/arthritis, factors that likely affected the performance of each individual bone.

Most individuals eligible for osteoporosis/osteopenia screening are not screened [25]. We found that most patients who have CT scans of the foot or ankle did not have a concurrent DXA scans. Therefore, there is a huge opportunity to identify patients who could benefit from a DXA scan after they have had a CT scan of the foot or ankle and are suspected to have decreased BMD based on our analysis. Similarly, patients with CT scans of the hand or wrist rarely have concurrent DXA scans, and even more rarely do they have concurrent CT scans of the foot or ankle, therefore our study is complementary to previously published studies using CT scans of the wrist and forearm, cervical spine, and chest to predict osteoporosis and osteopenia [26,30,31].

Our study has several clinical ramifications. First, the CT attenuations of the foot and ankle bones were not perfectly correlated. This may be because each bone has slightly different morphology and load-bearing capacity, and therefore the underlying trabecular structure may be different and as a result the CT attenuations are different. We also noted that the CT attenuations were not strongly correlated with the L1-L4 TBS, which suggests that the CT attenuation does not capture the same information contained in the L1-L4 trabecular bone scores. However, the CT attenuations were correlated with osteoporosis and osteopenia, which suggests that there is total body bone homeostasis, so that BMD loss at the hips or lumbar spine will be correlated with BMD loss at other bones, and therefore the CT attenuation at other bones. However, we hypothesize the degree to which BMD loss at the hips or lumbar spine correlates with the CT attenuation at other bones may depend on the biomechanical load these other bones are subject to, with bones that typically have smaller loads experiencing relatively more bone loss than bones that typically have higher loads. We showed that the CT attenuation of the calcaneus was best for predicting osteoporosis, which was expected, because estimates of BMD are often obtained at the calcaneus. Similarly, while the CT attenuation of the medial cuneiform was shown to be predictive of osteoporosis and osteopenia, it was not the most informative bone. Predictive machine learning models using clinical and demographic variables and CT attenuations at multiple osseous sites showed that SVMs with RBF kernels were best for predicting osteoporosis and osteopenia/osteoporosis.

To our knowledge, no studies have investigated the multivariable predictive power of the CT attenuations of the foot and ankle bones to diagnose osteoporosis. However, prior studies have shown that the calcaneus is a reasonable bone to use for screening for osteoporosis using ultrasound and quantitative CT [18]. Prior reports showed that the BMD measurements at different osseous sites were highly correlated [27,28], which would support our finding that the CT attenuations at different osseous sites are highly correlated. A prior study also showed that the TBS provides complementary information to DXA BMD measurements for prediction of fracture risk [29]. We found that although CT attenuations were correlated with the DXA BMD measurements, there were no significant correlations with the L1-L4 TBS, which suggests that

Table 4
Performance of the CT attenuation of each bone to predict osteoporosis and osteopenia/osteoporosis in the training/validation dataset.

Osteoporosis	CT attenuation threshold	Sensitivity	Specificity	AUC	Accuracy	Positive Predictive Value (PPV)	Negative Predictive Value (NPV)
Calcaneus	143.243	0.815	0.526	0.702	0.602	0.379	0.889
Talus	283.996	0.556	0.789	0.698	0.728	0.484	0.833
Navicular	298.246	0.741	0.697	0.700	0.709	0.465	0.883
Cuboid	127.220	0.667	0.605	0.634	0.621	0.375	0.836
Lateral cuneiform	264.602	0.852	0.513	0.686	0.602	0.383	0.907
Intermediate cuneiform	344.202	0.593	0.724	0.682	0.689	0.432	0.833
Medial cuneiform	260.755	0.667	0.605	0.644	0.621	0.375	0.836
SVM with linear kernel	–	0.778	0.750	0.819	0.757	0.525	0.905
SVM with RBF kernel	–	0.926	0.934	0.942	0.932	0.833	0.973
SVM with sigmoid kernel	–	0.630	0.539	0.568	0.563	0.327	0.804
PCA	–	0.444	0.934	0.689	0.748	0.510	0.963
Osteopenia/osteoporosis	**CT attenuation threshold**	**Sensitivity**	**Specificity**	**AUC**	**Accuracy**	**Positive Predictive Value (PPV)**	**Negative Predictive Value (NPV)**
Calcaneus	141.054	0.646	0.857	0.795	0.689	0.946	0.383
Talus	362.224	0.805	0.762	0.810	0.796	0.930	0.500
Navicular	372.465	0.829	0.667	0.767	0.796	0.907	0.500
Cuboid	139.161	0.659	0.714	0.708	0.670	0.900	0.349
Lateral cuneiform	311.144	0.854	0.667	0.808	0.816	0.909	0.538
Intermediate cuneiform	380.160	0.585	0.810	0.756	0.631	0.923	0.333
Medial cuneiform	327.331	0.890	0.571	0.740	0.825	0.890	0.571
SVM with linear kernel	–	0.878	0.857	0.888	0.874	0.960	0.643
SVM with RBF kernel	–	0.878	1.00	0.968	0.903	1.00	0.677
SVM with sigmoid kernel	–	0.695	0.524	0.570	0.660	0.851	0.306
PCA	–	0.951	0.524	0.738	0.864	0.886	0.733
Femoral neck BMD T-score ≤ -2.5	**CT attenuation threshold**	**Sensitivity**	**Specificity**	**AUC**	**Accuracy**	**Positive Predictive Value (PPV)**	**Negative Predictive Value (NPV)**
Calcaneus	116.188	0.692	0.722	0.705	0.718	0.264	0.942
Talus	281.738	0.538	0.744	0.631	0.718	0.233	0.918
Navicular	298.246	0.769	0.633	0.682	0.650	0.233	0.950
Cuboid	124.764	0.692	0.578	0.595	0.592	0.191	0.929
Lateral cuneiform	201.863	0.538	0.822	0.666	0.786	0.304	0.925
Intermediate cuneiform	424.880	0.923	0.378	0.631	0.447	0.176	0.971
Medial cuneiform	257.709	0.692	0.611	0.626	0.621	0.205	0.932
SVM with linear kernel	–	0.615	0.933	0.821	0.893	0.571	0.944
SVM with RBF kernel	–	0.923	0.989	0.964	0.981	0.923	0.989
SVM with sigmoid kernel	–	0.923	0.378	0.568	0.447	0.176	0.971
PCA	–	0.308	0.978	0.643	0.893	0.667	0.907
Femoral neck BMD T-score < -1	**CT attenuation threshold**	**Sensitivity**	**Specificity**	**AUC**	**Accuracy**	**Positive Predictive Value (PPV)**	**Negative Predictive Value (NPV)**
Calcaneus	122.043	0.543	0.970	0.775	0.680	0.974	0.500
Talus	349.638	0.786	0.636	0.750	0.738	0.821	0.583
Navicular	313.437	0.629	0.788	0.752	0.680	0.863	0.500
Cuboid	115.516	0.443	0.939	0.702	0.612	0.939	0.443
Lateral cuneiform	249.764	0.629	0.818	0.760	0.689	0.880	0.509
Intermediate cuneiform	380.160	0.643	0.788	0.748	0.689	0.865	0.510
Medial cuneiform	245.128	0.500	0.848	0.713	0.612	0.875	0.444
SVM with linear kernel	–	0.757	0.879	0.857	0.796	0.930	0.630
SVM with RBF kernel	–	0.786	0.970	0.923	0.845	0.982	0.681
SVM with sigmoid kernel	–	0.614	0.667	0.628	0.631	0.796	0.449
PCA	–	0.843	0.636	0.740	0.777	0.831	0.656

BMD, bone mineral density; SVM, support vector machine; RBF, radial basis function; PCA, principal components analysis.

trabecular bone scores may provide additional information on fracture risk beyond that predicted by the CT attenuations of trabecular bones.

We hypothesize that while all bones undergo bone loss with aging, some bones are preferentially targeted or affected. We believe the calcaneus may be affected prior to the talus. This would mean that on the spectrum of normal-osteopenia-osteoporosis, that the calcaneus would be best for differentiating osteoporosis from non-osteoporosis, while the talus would be better for differentiating osteopenia/osteoporosis from normal. However, we emphasize that this is just a hypothesis and further research is required to evaluate this hypothesis.

This study has a few limitations. First, the small sample size limits the power to detect small differences in AUC. We noted that very few patients had both CT scans of the foot and ankle and DXA scans within 1 year of each other. We anticipated that all patients older than 50 years of age with CT scans of the foot and ankle would have concomitant DXA scans, but the vast majority did not, which suggests there is insufficient screening for osteoporosis and osteopenia with DXA in our cohort as noted in prior studies [25]. Another challenge was that the field of view included on typical CT scans of the foot and ankle varied from patient to patient, limiting the ability to obtain CT attenuation measurements of the entire metatarsals, distal tibia, and fibula. As a result, we only analyzed the bones that were reliably visualized on all studies. Although semi-automatic segmentation of the bones is more accurate than fully automated segmentation, it was quite time consuming. However, as artificial intelligence research progresses, fully automated segmentation of each bone excluding the cortex, bone islands and other lesions that affect the CT attenuation of the bone will be completed, and this study can serve as a reference illustrating the correlations between the CT attenuations of the foot and ankle bones and osteoporosis and osteopenia. Our study only used an internal validation dataset (test dataset). An external validation

Table 5
Performance of SVM, PCA and CT attenuation threshold models in the test dataset.

Osteoporosis	Sensitivity	Specificity	AUC	Accuracy	Positive Predictive Value (PPV)	Negative Predictive Value (NPV)
CT attenuation threshold of 143.243 HU at the calcaneus	0.00	1.00	0.356	0.750	-	0.750
CT attenuation threshold of 260.755 HU at the medial cuneiform	0.667	0.578	0.622	0.600	0.345	0.839
SVM with RBF kernel	0.867	0.733	0.867	0.767	0.520	0.943
PCA model	0.533	0.933	0.733	0.833	0.727	0.857
Osteopenia/osteoporosis	**Sensitivity**	**Specificity**	**AUC**	**Accuracy**	**Positive Predictive Value (PPV)**	**Negative Predictive Value (NPV)**
CT attenuation threshold of 141.054 HU at the calcaneus	0.630	0.786	0.708	0.750	0.474	0.878
CT attenuation threshold of 327.331 HU at the medial cuneiform	0.00	1.00	0.318	0.767	-	0.767
SVM with RBF kernel	0.696	0.857	0.783	0.817	0.588	0.907
PCA model	0.913	0.357	0.635	0.483	0.302	0.941
Femoral neck BMD T-score ≤ -2.5	**Sensitivity**	**Specificity**	**AUC**	**Accuracy**	**Positive Predictive Value (PPV)**	**Negative Predictive Value (NPV)**
CT attenuation threshold of 116.188 HU at the calcaneus	0.625	0.731	0.678	0.717	0.263	0.927
CT attenuation threshold of 257.709 HU at the medial cuneiform	0.625	0.538	0.582	0.550	0.172	0.903
SVM with RBF kernel	0.875	0.635	0.750	0.667	0.269	0.971
PCA model	0.125	0.923	0.524	0.817	0.200	0.873
Femoral neck BMD T-score < -1	**Sensitivity**	**Specificity**	**AUC**	**Accuracy**	**Positive Predictive Value (PPV)**	**Negative Predictive Value (NPV)**
CT attenuation threshold of 122.043 HU at the calcaneus	0.00	1.00	0.382	0.400	-	0.400
CT attenuation threshold of 245.128 HU at the medial cuneiform	0.00	1.00	0.424	0.400	-	0.400
SVM with RBF kernel	0.972	0.500	0.766	0.783	0.745	0.923
PCA model	0.889	0.292	0.590	0.650	0.653	0.636

BMD, bone mineral density; SVM, support vector machine; RBF, radial basis function; PCA, principal components analysis.

dataset would be helpful to validate our findings. Finally, we noted that our study was not racially/ethnically diverse and further research needs to be done to evaluate how these results port to non-White populations.

In summary, opportunistic screening for osteoporosis and osteopenia/osteoporosis can be performed using the CT attenuation of the bones visualized from CT scans of the foot or ankle. If one had to pick a single bone to predict osteoporosis, then the CT attenuation of the calcaneus would be best with modest AUC of 0.702. However, if one used the CT attenuation of multiple bones then SVM analysis would be better than any single bone, and better than a PCA model. The benefit of using the CT attenuation of multiple bones is that these data all factor together in the analysis, mitigating the effect of any change in CT attenuation related to degenerative changes, fractures, or other focal bone changes.

CRediT author statement

Ronnie Sebro: Conceptualization, Formal analysis, Writing - Original Draft, Writing – Review & Editing.

Cynthia De la Garza-Ramos: Data curation, Writing - Review & Editing.

Conflicts of interest

The authors declare no competing interests.

Acknowledgments

RS was supported by R21 NIH/NIMH MH093415, United States.
ORCID Ronnie Sebro: 0000-0001-7232-4416. Cynthia De la Garza-Ramos: 0000-0002-6476-0397.

Appendix A. Supplementary data

Supplementary data to this article can be found online at https://doi.org/10.1016/j.afos.2022.09.002.

References

[1] Giles C. BMD predicts osteoporosis in recently postmenopausal women. Nat Rev Rheumatol 2006;2:294.
[2] Ahlborg HG, Johnell O, Turner CH, Rannevik G, Karlsson MK. Bone loss and bone size after menopause. N Engl J Med 2003;24:327–34.
[3] Management of osteoporosis in postmenopausal women: the 2021 position statement of the North American Menopause Society. Menopause 2021;28:973–97.
[4] O'Flaherty EJ. Modeling normal aging bone loss, with consideration of bone loss in osteoporosis. Toxicol Sci 2000;55:171–88.
[5] Newton JL, Jones DE, Wilton K, Pairman J, Parry SW, Francis RM. Calcaneal bone mineral density in older patients who have fallen. QJM 2006;99:231–6.
[6] Sekioka Y, Kushida K, Yamazaki K, Inoue T. Calcaneus bone mineral density using single Xx-ray absorptiometry in Japanese women. Calcif Tissue Int 1999;65:106–11.
[7] Mehta SD, Sebro R. Computer-aided detection of incidental lumbar spine fractures from routine dual-energy X-ray absorptiometry (DXA) studies using a support vector machine (svm) classifier. J Digit Imag 2020;33:204–10.
[8] Lewiecki EM. Bone densitometry and vertebral fracture assessment. Curr Osteoporos Rep 2010;8:123–30.
[9] Johansson H, Kanis JA, Oden A, Johnell O, McCloskey E. BMD, clinical risk factors and their combination for hip fracture prevention. Osteoporos Int 2009;20:1675–82.
[10] Hollevoet N, Verdonk R. Outcome of distal radius fractures in relation to bone mineral density. Acta Orthop Belg 2003;69:510–4.
[11] Ulivieri FM, Rinaudo L. Beyond bone mineral density: a new dual X-ray absorptiometry index of bone strength to predict fragility fractures, the bone strain index. Front Med 2021;7:590139.
[12] Viswanathan M, Reddy S, Berkman N, Cullen K, Middleton JC, Nicholson WK, et al. Screening to prevent osteoporotic fractures: updated evidence report and systematic review for the US Preventive Services Task Force. JAMA 2018;319:2532–51.
[13] Sözen T, Özışık L, Başaran NÇ. An overview and management of osteoporosis. Eur J Rheumatol 2017;4:46–56.
[14] Shevroja E, Cafarelli FP, Guglielmi G, Hans D. DXA parameters, Trabecular bone score (TBS) and bone mineral density (BMD), in fracture risk prediction in endocrine-mediated secondary osteoporosis. Endocrine 2021;74:20–8.
[15] Silva BC, Leslie WD, Resch H, Lamy O, Lesnyak O, Binkley N, et al. Trabecular bone score: a noninvasive analytical method based upon the DXA image. J Bone Miner Res 2014;29:518–30.
[16] Pickhardt PJ, Lee SJ, Liu J, Yao J, Lay N, Graffy PM, Summers RM. Population-based opportunistic osteoporosis screening: validation of a fully automated CT tool for assessing longitudinal BMD changes. Br J Radiol 2019;92:20180726.
[17] Wang P, She W, Mao Z, Zhou X, Li Y, Niu J, et al. Use of routine computed tomography scans for detecting osteoporosis in thoracolumbar vertebral bodies. Skeletal Radiol 2021;50:371–9.

[18] Yen C-C, Lin W-C, Wang -TH, Chen G-F, Chou D-Y, Lin D-M, et al. Pre-screening for osteoporosis with calcaneus quantitative ultrasound and dual-energy X-ray absorptiometry bone density. Sci Rep 2021;11:15709.
[19] Baroncelli G. Quantitative ultrasound methods to assess bone mineral status in children: technical characteristics, performance, and clinical application. Pediatr Res 2008;63:220–8.
[20] Fedorov A, Beichel R, Kalpathy-Cramer J, Finet J, Fillion-Robin J-C, Pujol S, et al. 3D slicer as an image computing platform for the quantitative imaging network. Magn Reson Imaging 2012;30:1323–41.
[21] Elangovan SM, Sebro R. Accuracy of CT attenuation measurement for differentiating treated osteoblastic metastases from enostoses. Am J Roentgenol 2018;210:615–20.
[22] Nicolaou S, Liang T, Murphy DT, Korzan JR, Ouellette H, Munk P. Dual-energy CT: a promising new technique for assessment of the musculoskeletal system. Am J Roentgenol 2012;199(5 Suppl):S78–86.
[23] Panchbhavi VK, Boutris N, Patel K, Molina D, Andersen CR. CT density analysis of the medial cuneiform. Foot Ankle Int 2013;34:1596–9.
[24] Cohen A, Foldes AJ, Hiller N, Simanovsky N, Szalat A. Opportunistic screening for osteoporosis and osteopenia by routine computed tomography scan: a heterogeneous, multiethnic, middle-eastern population validation study. Eur J Radiol 2021;136:109568.
[25] Majumdar SR, Leslie WD. Conventional computed tomography imaging and bone mineral density: opportunistic screening or "incidentaloporosis"? Ann Intern Med 2013;158:630–1.
[26] Sebro R, De la Garza-Ramos C. Machine learning for opportunistic screening for osteoporosis from CT scans of the wrist and forearm. Diagnostics 2022;12:691.
[27] Mehta SD, Sebro R. Random forest classifiers aid in the detection of incidental osteoblastic osseous metastases in DXA studies. Int J Comput Assist Radiol Surg 2019;14:903–9.
[28] Sebro R, Ashok SS. A statistical approach regarding the diagnosis of osteoporosis and osteopenia from DXA: are we underdiagnosing osteoporosis? JBMR Plus 2021;5:e10444.
[29] Harvey NC, Glüer CC, Binkley N, McCloskey EV, Brandi ML, Cooper C, et al. Trabecular bone score (TBS) as a new complementary approach for osteoporosis evaluation in clinical practice. Bone 2015;78:216–24.
[30] Sebro R, De la Garza-Ramos C. Utilizing machine learning for opportunistic screening for low BMD using CT scans of the cervical spine. J Neuroradiol 2022. https://doi.org/10.1016/j.neurad.2022.08.001. In press.
[31] Sebro R, De la Garza-Ramos C. Machine learning for the prediction of osteopenia/osteoporosis using the CT attenuation of multiple osseous sites from chest CT. Eur J Radiol 2022;155:110474. https://doi.org/10.1016/j.ejrad.2022.110474. In press.